CHAPTER-3

EXPERIMENTAL PROCEDURE

The current chapter describes the details of the material and the method used for creating textures on the surface of bearing steel which is followed by a brief description of the techniques used for the characterization of dimples. The chapter also highlights the procedure and the parameters undertaken to examine the tribological behaviour of textured steel under dry as well as lubricated conditions. The techniques used for the analyses of worn surfaces are also included in the chapter.

3.1 PROCUREMENT OF MATERIAL

The cylindrical rods of bearing steel (AISI52100) of 60 mm diameter procured from All India Metal Corporation, Mumbai, have been used in the present investigation.

3.2 DETERMINATION OF CHEMICAL COMPOSITION

The chemical composition of bearing steel (AISI52100) used in the present study has been determined through energy-dispersive X-ray spectroscopy (51N1000 – EDS System, Oxford Instruments Nanoanalysis), and the results are presented in Chapter 4.

3.3 SAMPLE PREPARATION

The circular disc-shaped (ϕ 50 mm × 5 mm) bearing steel specimens have been prepared by cutting and turning operations on the lathe in the Central Workshop of IIT (BHU), Varanasi. The cylindrical pins to be used as counter specimens (ϕ 5.7 mm × 45 mm) have also been machined by cutting and turning operations on the lathe and with the edges chamfered

(0.5 mm×45°) and the same is shown in Fig. 3.1. The discs and faces of pins have been polished with different grades of emery papers (80#, 120#, 220#, and 400#, 600# and 800# respectively) followed by cloth polishing using the diamond paste to obtain a smooth and mirror finish bright surface and initial surface roughness of R_a = 0.04µm.

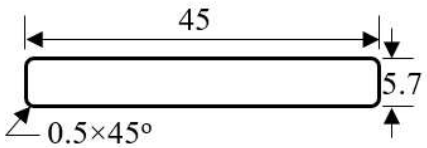

Fig. 3.1 Schematic diagram of counterface pin (all dimensions in mm)

The surface roughness of the polished specimens has been measured by a noncontact 3D optical surface profiler (Zygo NexView, AMETEK Inc., USA). The discs have been cleaned in an ultrasonic bath with acetone and ethanol for about 15 minutes each to remove the surface impurities, dust, oil, oxides layer, and any other contamination left during sample preparation. These discs were further used as untextured samples for the purpose of reference, and some of the discs were textured by laser surface texturing.

3.4 LASER SURFACE TEXTURING

In the present study, the discs were textured with circular and bi-triangular-shaped dimples shown in Fig.3.2 on the disc surface with two different densities. The area of bi-triangular dimples has been calculated assuming a straight edge for simplicity; however, in practice, the edges are slightly curved. The total number of dimples, *N*, can be calculated by the relation given in Eqn. (3.1) given below.

$$N = \frac{A_{disc}}{a_{dimple}} \times \ Area\ Density \tag{3.1}$$

Area of the disc, $A_{disc} = \frac{\pi D^2}{4}$, (3.2)

Area of a single dimple, $a_{dimple} = \begin{cases} \frac{\pi d^2}{4}, for\ circular\ dimple \\ l^2/_2, for\ bi-triangular\ dimple \end{cases}$ (3.3)

Where, *D* is the diameter of the disc, *d,* is the diameter of the circular dimple, and *l* is the diagonal distance between corners of the bi-triangular dimple, as shown in Fig. 3.2.

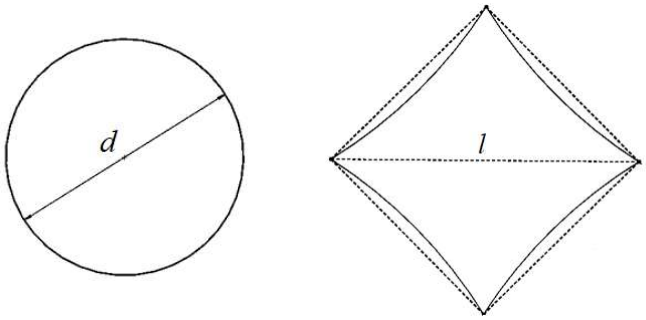

(a) A circular dimple (b) A bi-triangular dimple

Fig. 3.2 Shapes of dimples used in the study

Figure 3.3 illustrates a schematic sectional view of two surfaces in conformal contact with relative motion (*U*) between them, one of which is partially textured. The gap between the contacting surfaces due to the presence of the lubricant film can be given by *h(x, z)* as shown in Fig. 3.3.

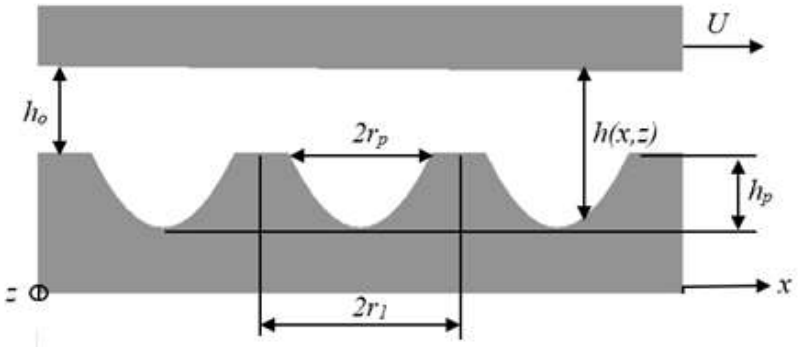

Fig. 3.3 Film thickness and geometry of micro-dimples

Micro-dimple aspect ratio = $h_p/2r_p$

Where, h_p is the maximum depth of a micro-dimple, r_p is the maximum size (or radius in case of a circular dimple) of the micro-dimple, h_o is the gap between the surfaces away from the dimple, $2r_1$ is the side of an imaginary square in the centre of which each dimple is located and (x_c, z_c) is the centre of the dimple in XZ plane.

Figure 3.4 shows the cross-section of a single dimple. The depth of the dimple can be approximated by the relation given in Eqn.3.4.

$$-\left(\frac{h_p}{r_p^2}\right)r^2 + h_p, above\ the\ recess\ or\ when\ r \le r_p, where\ r = \sqrt{(x-x_c)^2 + (z-z_c)^2} \quad (3.4)$$

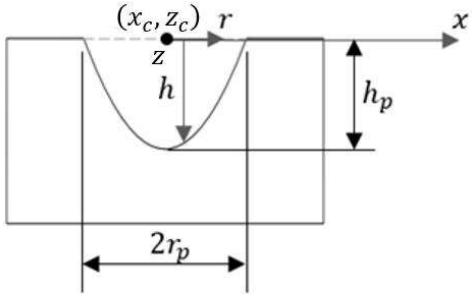

Fig. 3.4 Cross-sectional profile of a single dimple

In the present case, the shape is bi-triangular, and the edges have been slightly curved. The curved edges are longer than the straight edges to allow for the trapping of worn particles and the easy flow of oil into the cavity during lubrication testing. The variation in the depth of the dimple and gap between the contacting surfaces can be thus approximated by the expressions given in Table 3.1 for circular as well as bi-triangular dimples. The surface texturing parameters employed in this study are shown in Table 3.2.

Table 3.1 Analytical description of cross-sectional profile for textures

Shape	Depth	Gap between the contacting surfaces
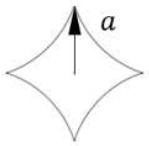	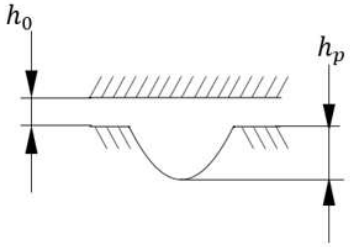	$h = \begin{cases} h_0, & when\ r > a \\ -\left(\frac{h_p}{a^2}\right) r^2 + h_p + h_o, & when\ r \le a \end{cases}$ $where, a = {}^{l}/_{2};\ r = \sqrt[n]{(x - x_c)^n + (z - z_{c)}{}^n};\ n < 1$
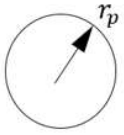	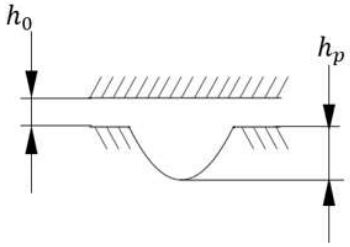	$h = \begin{cases} h_0, & when\ r > r_p \\ -\left(\frac{h_p}{r_p^2}\right) r^2 + h_p + h_o, & when\ r \le r_p \end{cases}$ $where, r = \sqrt{(x - x_c)^2 + (z - z_c)^2}$

Where, a is the half of the diagonal length (l) of the bi-triangular dimple, n is the exponent. The exponent n should be smaller than 1, which in the present case is around 0.88.

Table 3.2 Surface texturing parameters

Material		AISI 52100	
Dimensions		ϕ 50×5 mm	
Surface		Both surfaces polished, R_a 0.04-0.1 µm,	
		Chamfering 0.5mm×45°	
Texturing			
Geometry		Area Density, (or Pit area ratio) %	Array
Bi-triangular	0.5 mm (l), 8 µm depth	7, 20	Spiral
Circle	ϕ 0.5 mm (d), 8 µm depth	7, 20	

CAD models of specimens shown in Fig. 3.5 (a through d), corresponding to circular- and bi-triangular-shaped dimples having and 7 and 20% density, respectively, for each, were created using SOLIDWORKS 2018 and saved in .dxf format, which was further used as input

for laser surface texturing. DXF is an exchange format for the content of CAD drawing files (DWG).

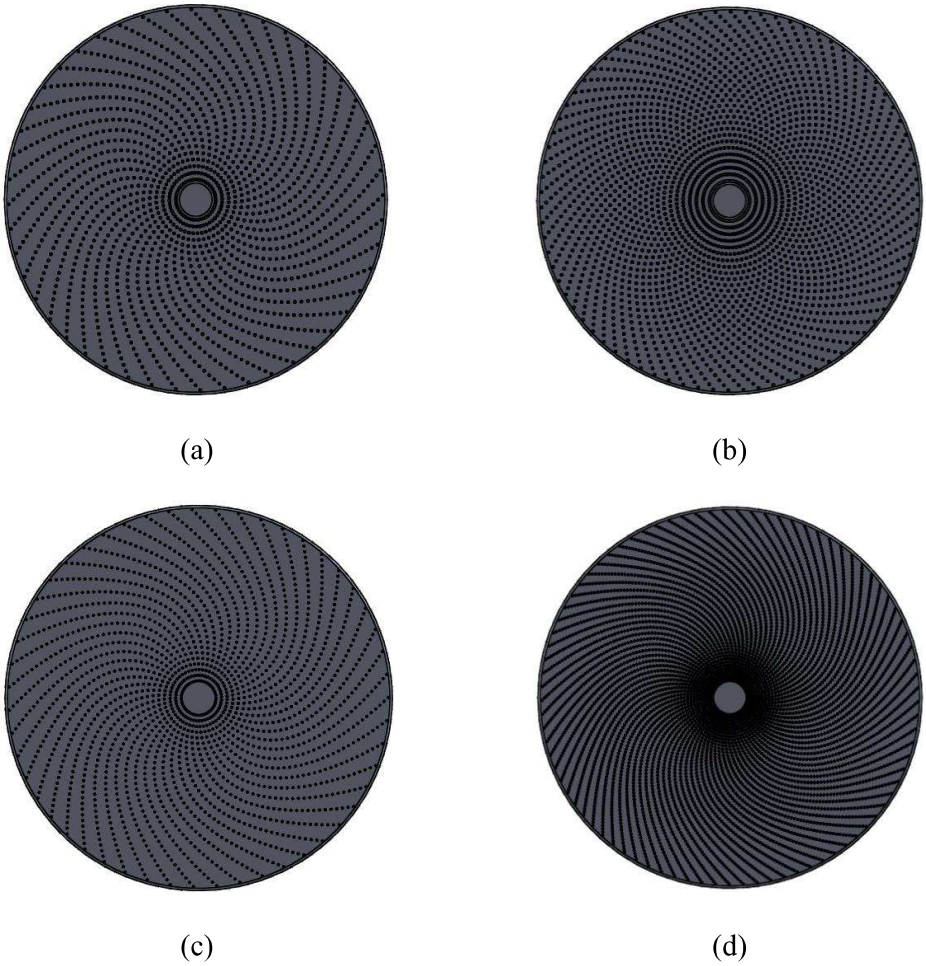

(a) (b)

(c) (d)

Fig. 3.5 CAD images of the discs textured with a spiral array of (a) circular dimples, density 7%, (b) circular dimples, density 20%, (c) bi-triangular, density 7%, and (d) bi-triangular, density 20%.

Before texturing, the polished disc specimens were ultrasonicated in acetone and rinsed with isopropyl alcohol. Nanosecond pulse Nd:YAG fibre laser with a maximum laser power of 20 W, the wavelength of 1064 nm with one ablation, and two finishing passes were used to produce dimples of specific shapes and array on the surface of steel discs by using the CAD input file. Laser texturing was done at LASER JOB WORK, Noida, India. Table 3.3 presents the laser texturing parameters. The textured specimens have been designated on the

basis of the shape, and the density of dimples like the specimens textured with circular shape dimples and 7% & 20% density have been named as CT7 and CT20, whereas those with bi-triangular dimples with 7 % and 20% are designated as BT7 and BT20.

Table 3.3 Laser surface texturing parameters

	Pass 1	**Pass 2**	**Pass 3**
Speed, mm/s	200	1000	1000
Power, W	16	8	6
Frequency, kHz	40	55	65

3.5 CHARACTERIZATION OF DIMPLES

The textured surfaces are examined under an optical microscope (Dewinter Inverted Metallurgical Microscope, Model: DMI Premium) and scanning electron microscope (SEM; EVO 18, Carl Zeiss Microscope). Topographies and profiles of dimples have been analyzed using a non-contact 3D optical profilometer integrated with a multifunctional tribometer (Rtec Instruments, USA). The inline optical 3D profilometer comes with a six-objective manual or automatic turret that can accommodate several objectives and a user-selectable four-color high-brightness LED light source. It has a low-noise camera unit and professional data analysis software. Each lens comes with calibration and inspection settings on the tester and an image test area with nm resolution with high-precision z-motion control. The software allows computing both line and area roughness. Calculation of nearly all ASME, ISO, and DIN surface roughness parameters can be done.

3.6 FRICTION AND WEAR TESTING

Friction and wear tests have been performed on untextured and textured specimens using a pin-on-disc rotary tribometer (DUCOM, Bengaluru, India) according to standard test methods of ASTM G99. The sliding tests have been conducted in dry and wet conditions against a pin of 100Cr6 steel having a flat face with rounded corners (Fig. 3.1) to have a self-mated conformal contact. The mass loss after a predetermined number of cycles was measured by the difference in the mass of specimens before and after the tests. An electronic weighing balance having an accuracy of 10^{-7} kg was used for measuring the mass loss, which was then converted to volume loss by dividing it by the density of the specimen. Each specimen under a set of experimental conditions has been tested thrice to minimise the experimental error, and the average value has been reported. Friction force was recorded in the computer through DUCOM Software through the data acquisition system having an interface with the tribometer. The tangential friction force is continuously displayed by the friction and wear monitor as the rubbing between the specimen pin and counterface begins. The friction force is recorded and used to calculate the coefficient of friction using the following formula given in Eqn. (3.5).

$$\text{Coefficient of friction: } \mu = \frac{F}{N} \tag{3.5}$$

where F = friction force, N= normal force.

3.6.1 DRY CONDITION

The friction and wear behaviour of textured specimens was investigated using the pin-on-disc rotary tribometer at room temperature, with relative humidity in the range of 45-55% under unidirectional sliding against the bearing steel pin of 5.7 mm diameter. In order to evaluate the friction and wear performance under unidirectional sliding, the disc has been set to rotate against the stationary counterpart (pin) with the testing conditions given in Table 3.4.

Table 3.4 Experimental conditions used for investigating the tribological performance under dry conditions

Specimen		WTD (mm)	Speed (m/s)	Number of Revolutions	Normal Load (N)
Untextured		14, 24, 34, 44	0.2, 0.6, 1.0	8000	15, 30
Textured	CT7	14, 24, 34, 44	0.2, 0.6, 1.0	8000	15, 30
	CT20	14, 24, 34, 44	0.2, 0.6, 1.0	8000	15, 30
	BT7	14, 24, 34, 44	0.2, 0.6, 1.0	8000	15, 30
	BT20	14, 24, 34, 44	0.2, 0.6, 1.0	8000	15, 30

The friction and wear behaviour of untextured and textured bearing steels have been investigated for 8000 revolutions. The mass loss of both the disc and the counterface pin has been measured before and after the tests. The volume is calculated by dividing the measured weight loss by the density of the material. Further, the wear rate, W, has been calculated using Eqn. (3.6) as given below:

$$W = \frac{V}{L} \tag{3.6}$$

Where, V, and L are the total wear volume, and the total sliding distance, respectively.

The coefficient of friction during each run has been recorded through a data acquisition system in a computer that had an interface with the tribometer. The data from the starting to end of the test has been used to estimate the average coefficient of friction.

3.6.2 LUBRICATED CONDITION

Sliding wear tests have also been performed on textured specimens using the pin-on-disc tribometer under lubricated conditions. The counterface pin of 100Cr6 steel has a flat face

with rounded corners (0.5mm × 45°) to ensure conformal contact. The sliding tests are conducted at different normal loads of 10, 30 and 50 N and sliding speeds of 0.2, 0.8, 1.4 and 2.0 m/s against the 5.70 mm diameter pin for 8000 revolutions. The tests have been performed in atmospheric air with a room temperature of 30 ± 2 ^{0}C and relative humidity in the range of 45-55% under the lubricated condition on an open system by using fresh oil on each new sliding track. Before each test, a single drop (approximately 27μL, concentrations lower than 1.05×10^{-3} ml/mm^2) of commercial multigrade oil (LIQUIMOLY fully synthetic high-performance gear oil 75W- 90) is applied between the sliding surfaces with no further addition of lubricant during the test. It is high-pressure, low-viscosity gear oil used in the transmission system. Table 3.5 lists the details of experimental conditions adopted for testing under lubricated conditions whereas the properties of the lubricating oil are presented in Table 3.6.

Table 3.5 Experimental conditions used for investigating the tribological performance under lubricated conditions

Tribo-element		Motion			Pin Load (N)
		WTD (mm)	Speed (m/s)	Number of Revolutions	
Untextured		14, 24, 34, 44	0.2, 0.8, 1.4, 2	8000	10, 30, 50
Textured	CT7	14, 24, 34, 44	0.2, 0.8, 1.4, 2	8000	10, 30, 50
	CT20	14, 24, 34, 44	0.2, 0.8, 1.4, 2	8000	10, 30, 50
	BT7	14, 24, 34, 44	0.2, 0.8, 1.4, 2	8000	10, 30, 50
	BT20	14, 24, 34, 44	0.2, 0.8, 1.4, 2	8000	10, 30, 50

Table 3.6 Physical properties of oil used for testing

Oil	Specific Gravity	Pour Point, °C	Flash Point, °C	Kinematic Viscosity, cSt at

				40 °C	100 °C
Low Viscosity Oil (SAE 75W-90)	0.855	-60	200	81.5	14.3

The friction coefficient has been used to determine the operating lubrication regime in the current investigation. Load and speed have been changed throughout each test which have an effect on the lubricant film thickness and hence the lubrication regime. Although the friction coefficient was continuously measured and recorded during each test, steady average friction coefficient data are utilised to assess the lubrication regime.

In order to determine the duration (number of cycles) of the effectiveness of dimples, tests for longer runs have also been conducted at different speeds and a sudden increase in friction coefficient has been considered as the effective lifetime of the dimples. The increase in the coefficient of friction after a certain number of revolutions has been considered as the loss in effectiveness of the dimples.

3.7 EXAMINATION OF WORN SURFACES

The topographies and profiles of the surfaces worn under different conditions of sliding, i.e., dry and lubricated under different loads and speeds, have been examined under non-contact 3D optical profilometer integrated with a multifunctional tribometer (Rtec Instruments, USA). The worn tracks on the discs have also been analysed under a scanning electron microscope (SEM; EVO 18, Carl Zeiss Microscope) equipped with an energy-dispersive X-ray spectroscopy (51N1000 – EDS System, Oxford Instruments Nano-analysis) to explore the probable mechanisms of wear.